

All

Q

ADVANCED SEARCH

Conferences > 2017 International Conference...

A Novel Testing Method for Narrowband Synthetic Aperture Radar (SAR) Imaging Algorithm

Publisher: IEEE

Cite This

PDF

Letian Zeng ; Chunhui Yang ; Yuelong Zhao ; Ping Chen ; Qiang Wang All Authors

88 Full Text Views



Abstract

Document Sections

I. Introduction

II. Proposed Testing Method Based on Flow Path

III. Experimental Results

IV. Conclusion

Authors

Figures

References

Keywords

Metrics

Abstract: Imaging algorithms are the key factors of the performances of the synthetic aperture radar (SAR) imaging. Most existing methods usually need to utilize field environment and data, which dramatically reduces the effectiveness of the software testing. This paper presents a novel testing method for narrow-band SAR imaging algorithms, which is consisted of four parts: system parameter verification, echo data simulation, algorithm simulation and real data verification, evaluations of imaging results. This scheme has fully validated the correctness and feasibility of imaging algorithms. Also, this approach greatly improves the validity of the testing work. Finally, the correctness and effectiveness of the proposed method are verified by simulation experiments and real data results.

Published in: 2017 International Conference on Dependable Systems and Their Applications (DSA)

Date of Conference: 31 Oct.-2 Nov. 2017 **INSPEC Accession Number:** 17541218

Date Added to IEEE Xplore: 25 January 2018 **DOI:** 10.1109/DSA.2017.19

Publisher: IEEE

Conference Location: Beijing, China

ISBN Information:
Electronic ISBN:978-1-5386-3690-9
Print on Demand(PoD)
ISBN:978-1-5386-3691-6

Need Full-Text

access to IEEE Xplore for your organization?

CONTACT IEEE TO SUBSCRIBE >

More Like This

Plug-and-Play Synthetic Aperture Radar Image Formation Using Deep Priors
IEEE Transactions on Computational Imaging
Published: 2021

Multifrequency Compressed Sensing for 2-D Near-Field Synthetic Aperture Radar Image Reconstruction
IEEE Transactions on Instrumentation and Measurement
Published: 2017

Show More

THE IEEE APP:

Let's stay connected...

DSA 2017

Fourth International Conference on Dependable Systems and Their Applications

31 October - 2 November 2017 • Beijing, China



Technical Sponsor
IEEE Reliability Society

Sponsor
Technology & Engineering Center for Space Utilization, CAS

Co-Sponsors
Key Laboratory of Space Applications, CAS
Institute of Automation, CAS
The Twentieth Research Institute, China Electronic Technology Group Corporation
AVIC Chengdu Aircraft Design and Research Institute
Dalian University of Technology
Wuhan University of Technology

CONFERENCE INFORMATION

PAPERS BY SESSION

PAPERS BY AUTHOR

GETTING STARTED

TRADEMARKS

SEARCH

Fourth International Conference on Dependable Systems and Their Applications DSA 2017

Table of Contents

Message from the General Chair.....	ix
Message from the Program Chairs	x
Organizing Committee.....	xi
Program Committee.....	xii
Conference Supporters.....	xiii
Opening and Keynote Speeches	xiv

Session: Formal Methods and Testing

Mutation Testing Based Evaluation of Formal Verification Tools	1
<i>A. Chakrapani Rao, A. Raouf, G. Dhadyalla, and V. Pasupuleti</i>	
A Method of False Alarm Recognition Based on k-Nearest Neighbor	8
<i>Fei Guan, Junyou Shi, Xiaodong Ma, Weiwei Cui, and Jie Wu</i>	
Formalization of Laplace Transform in Coq	13
<i>Yifei Wang and Gang Chen</i>	
A New Attribute Selection Method Based on Maximal Information Coefficient and Automatic Clustering	22
<i>Haijin Ji, Song Huang, Yaning Wu, Zhanwei Hui, and Xuewei Lv</i>	

Session: Security and Dependable System

A System Safety Analysis Method Based on Multiple Category Hazard Factors	29
<i>Hao Wang, Deming Zhong, Yukun Zhao, and Rui Sun</i>	
CVSSA: Cross-Architecture Vulnerability Search in Firmware Based on Support Vector Machine and Attributed Control Flow Graph	35
<i>Hong Lin, Dongdong Zhao, Linjun Ran, Mushuai Han, Jing Tian, Jianwen Xiang, Xian Ma, and Yingshou Zhong</i>	

An Experimental Study of Four Methods for Homology Analysis of Firmware Vulnerability	42
<i>Linjun Ran, Liping Lu, Hong Lin, Mushuai Han, Dongdong Zhao, Jianwen Xiang, Haiguo Yu, and Xian Ma</i>	
Software Architecture Modeling and Reliability Evaluation Based on Petri Net	51
<i>Chi Zhang, Yunyun Ma, Xiaohua Wang, and Ruixue Wang</i>	

Session: Data Processing and Applications

Plaintext-Dependent Selective Image Encryption Scheme Based on Chaotic Maps and DNA Coding	57
<i>Lin Li, Yingying Yao, and Xiaolin Chang</i>	
A Novel Testing Method for Narrowband Synthetic Aperture Radar (SAR) Imaging Algorithm	66
<i>Letian Zeng, Chunhui Yang, Yuelong Zhao, Ping Chen, and Qiang Wang</i>	
Prediction of Cancer Based on Mobile Cloud Computing and SVM	73
<i>Liang Kou, Ye Yuan, Jianguo Sun, and Yun Lin</i>	
A Software Defined Work Based Approach to Dependable Scenic Region Management	77
<i>Hongming Che, Lin Zou, Qinyun Liu, Sicong Ma, Hongji Yang, Chi Zhang, William Chengchung Chu, and Haiying Qi</i>	

Session: Fault Diagnosis

High-Reliable Testing for FPGA Software in Space Utilization Engineering	86
<i>Tao Zhang and Xiaodan Wang</i>	
System Analysis and PHM Methods for Power Devices Based on Physics-of-Failure	92
<i>Yulong Zhang, Lulu Wang, Bo Gao, Lixin Wang, Jiajun Luo, and Zhengsheng Han</i>	
A Fault Diganosis Method Based on Bispectrum-LPP and PNN	98
<i>JinLong Zhao, Pinwang Zhao, Shulin Liu, Yue Liu, Qiufang Wang, and Na Jiao</i>	

Session: Software Design and Testing

Anomaly Detection Method of Space Payload Using Multivariate State Estimation Technique and Self-Organizing Feature Map	103
<i>Lei Song, Lili Guo, Huiping Wang, Shilong Yang, Shan Jin, Jiangyong Duan, and Lele Xu</i>	
Performance Analysis Model for Fog Services under Multiple Resource Types	110
<i>Bo Liu, Xiaolin Chang, Bing Liu, and Zhi Chen</i>	
Deterministic Replay for Multi-Core VxWorks Applications	118
<i>Junjie Liu, Xiaopeng Gao, Bo Jiang, Shunkun Yang, and Zhenyu Zhang</i>	

Poster Papers

The Timed Abstract State Machine Based Test Data Auto Generation for Embedded Systems	126
<i>Zhexi Yao, Tao Zhang, Tao Zhang, and Jinbo Wang</i>	
Formal Derivation and Verification of Coordinate Transformations in Theorem Prover Coq	127
<i>Zhenwei Ma and Gang Chen</i>	
Extend STPA Method Using Hybrid Dynamic Theory	137
<i>Zhe Li, Deming Zhong, Rui Sun, and Hao Wang</i>	
Test Cases Generation for Multiple paths Based on Metamorphic Relation	143
<i>Xuewei Lv, Song Huang, Zhanwei Hui, Haijin Ji, and Shan Li</i>	
A Software Reliability Test Suite Generating Approach Based on Hybrid Model for Complex Equipment System	144
<i>Li Yin, Sun Zhi-An, and Jiang-Ting-Ting</i>	
A Novel Approach for Coverage Probing of Embedded Software in SoPC	155
<i>Lu Kong, Bin Wang, Shan Zhou, and YaWen Yang</i>	
Cross Clock Domain Signal Research Based on Dynamic Motivation Model	156
<i>Shan Zhou, Tao Zhang, and YaWen Yang</i>	
Testing Requirement Analysis Method Based on Signal Path for High Reliability Software	157
<i>Yunyun Ma, Jinbo Wang, Yuelong Qu, and Tao Zhang</i>	
A Software Reliability Model Based on Failure Mode	158
<i>Feng Er-Qiang and Zheng Jun</i>	
Comprehensive Evaluation of Software Quality Based on LM-BP Neural Network	162
<i>Anbang Wang, Lihong Guo, Yuan Chen, Junjie Wang, and Yuanzhang Song</i>	
On the Evaluation Metrics of Automated Program Repair	168
<i>Yuhua Qi, Wenhong Liu, Weixiang Zhang, and Deheng Yang</i>	
A Three-Stage Defect Prediction Model for Cross-Project Defect Prediction	169
<i>Song Huang, Yaning Wu, Haijin Ji, and Chengzu Bai</i>	
Error Analysis and Correction of Time-Frequency Synchronization Based on Packet Switching	170
<i>Wei Wei, Zhong Hongen, and Cao Suzhi</i>	
Improved Fault Diagnosis Method for Power Systems Based on Grey System Theory	171
<i>Jianmin Wang, Jinbo Wang, and Bin Wang</i>	

Efficient Keyword Search over Online Social Network by Using Stream Dynamic Bloom Filter	172
<i>Jinzhou Huang, Zhekun Hu, and Zheng Dai</i>	
Improved Evidence Conflict Measurement Algorithm Based on Singular Value Decomposition	178
<i>Xinglin Guo, Yunqiang Yan, Lianzhi Qi, Yi Zhang, and Quangen Chen</i>	
An Extendibility Analysis Method Research for Integrated Test Diagnosis on Ship Complex System	179
<i>Fei Li, Bai Liu, Di Peng, and Longli Tang</i>	
Author Index	180

A Novel Testing Method for Narrowband Synthetic Aperture Radar (SAR) Imaging Algorithm

Letian Zeng
Software Quality Engineering
Research Center
CEPREI
GuangZhou, China
zengletian@ceprei.com

Chunhui Yang
Software Quality Engineering
Research Center
CEPREI
GuangZhou, China
yangch@ceprei.com

Yuelong Zhao
School of Computer and
Engineering
South China University of
Technology
GuangZhou, China
ylzhao1@scut.edu.cn

Pin Chen
Software Quality Engineering
Research Center
CEPREI
GuangZhou, China
chenping@ceprei.com

Qiang Wang
Software Quality Engineering
Research Center
CEPREI
GuangZhou, China
cptester@163.com

Abstract—Imaging algorithms are the key factors of the performances of the synthetic aperture radar (SAR) imaging. Most existing methods usually need to utilize field environment and data, which dramatically reduces the effectiveness of the software testing. This paper presents a novel testing method for narrow-band SAR imaging algorithms, which is consisted of four parts: system parameter verification, echo data simulation, algorithm simulation and real data verification, evaluations of imaging results. This scheme has fully validated the correctness and feasibility of imaging algorithms. Also, this approach greatly improves the validity of the testing work. Finally, the correctness and effectiveness of the proposed method are verified by simulation experiments and real data results.

Keywords—Synthetic aperture radar (SAR) imaging, algorithm testing, echo data simulation, algorithm simulation and real data verification, evaluations of imaging results.

I. INTRODUCTION

Synthetic aperture radar (SAR) [1-3] can obtain high resolution in the range dimension by transmitting wideband linear frequency modulation signals and achieve high resolution in the azimuth dimension via a long azimuth time accumulation, forming a two-dimension high-resolution SAR image about the electromagnetic information of illuminated scene. Generally, SAR imaging algorithms are mainly consisted of two kinds: frequency domain algorithms and time domain algorithms. Frequency domain algorithms have almost the same processing ideas, such as range cell walk correction and second range compression [1]. Then, azimuth compression [2] is performed using fast Fourier transform (FFT). Time domain algorithms remove the range-azimuth coupling through energy accumulation along the range track of the target to implement focusing in the azimuth. Besides, the imaging plane of frequency domain algorithms is the slant plane and the algorithms are susceptible to the effects of radar working frequency as well as processing accuracy. While, time domain

algorithms can choose the imaging plane randomly, without being limited by radar working frequency.

As the key factors in the SAR signal processing module, SAR imaging algorithms usually have a significant influence on the performances of SAR systems. Testing [4-7] for the imaging algorithms is a crucial means to guarantee the efficiency of the systems. The approximations within the imaging algorithms probably have indirect effects on the effective scope of the illuminated scene and the final focusing results, which cannot be deduced by accurate expressions and should take consistent steps to test for different occasions to find out defects deeply hidden in the algorithms. However, the study on the algorithm testing is rather rare. What's more, testers often check the echo signals in data acquisition with the help of field radar data playback software, providing effective history data for signal processing. When carrying out configuration item test, testers print out the real output data according to the debugging environment and compare the results with the theoretical values achieved by certain simulation software, like Matlab. That is, testers have to resort to the field equipment, data and environment, which makes it difficult to keep the independence of testing work [8-13]. Furthermore, in the system test, testers often intuitively observe the imaging results of targets to judge their performances and give preliminary conclusions, but they lack concrete evaluating methods as well as evaluating indicators to analyze the image resolution, focusing performance together with focusing position. This results in incomplete verifications of imaging algorithms in many conditions, making the testing for the algorithms not thorough and dramatically reducing the feasibility of the testing work.

To deal with these problems, this paper presents a novel testing method based on flow path, comprehensively validating the correctness of narrowband SAR imaging algorithms in the broadside mode from the following four aspects: system parameter verification, SAR echo simulation [14,15],

simulation of SAR imaging algorithm and verification of real SAR data, evaluation of SAR imaging results. The proposed method improves the effectiveness of the testing work, providing theoretical and practical guidance for radar software testing. Firstly, we give the SAR system parameter design attentions. Then, the improved concentric circle method (ICCM) [14] is employed to flexibly configure the system parameters and rapidly generate the SAR echo data. The back projection (BP) algorithm is applied to process the SAR data and the image quality is analyzed according to the imaging results, without relying on field echo data. Besides, associated problems in implementing different algorithms are investigated and verified by imaging algorithm simulation and real data processing. To improve the effectiveness of software testing, we introduce reasonable and quantizable indicators to evaluate the whole focusing performance as well as the local focusing property of some certain point targets for the SAR imaging results, rather than roughly estimate them just by observing. Finally, the correctness and effectiveness of the proposed method are validated by simulation experiments and real data results.

II. PROPOSED TESTING METHOD BASED ON FLOW PATH

In this part, we propose a novel testing method based on flow path for narrowband SAR imaging algorithm, including four steps: (1) the verification of system parameter design, (2) SAR echo simulation, (3) simulation of SAR imaging algorithm and verification of real SAR data, (4) evaluation of SAR imaging results. Through this flow path, we can comprehensively verify the performance of the broadside SAR imaging algorithms.

A. Verification of System Parameter Design

Many factors should be taken into account when we perform the SAR system parameter verification, such as beam width, scope of the illuminated scenario, resolution of a SAR image and the selection of pulse repeat frequency (PRF). Hence, we should ensure that the associated parameters satisfy the design requirement, especially the bandwidth, sampling rate and numbers in the range dimension as well as the coherent integration time. Also, the Doppler bandwidth should be less than PRF value to avoid the spectrum folding. Generally speaking, extra margins are retained when developers design system parameters. Moreover, system parameters are subject to SAR platforms—different factors are taken into consideration for airborne SAR, satellite SAR together with missile-borne SAR. For example, when dealing with missile-borne SAR parameter design, the influences of singularity echo restrictions are key factors.

B. SAR Echo Simulation

In general, independent testing environment and testing data are needed for radar software testing. To validate SAR imaging algorithms effectively and get rid of the field SAR echo data, the SAR echo simulation becomes a necessity. In this paper, the ICCM are employed to promisingly improve the computing efficiency of generating simulation data, producing both point target echoes and distributed scene target echoes

with a high accuracy and a fast speed [14,15]. The distributed scene targets refer to a collection of point targets with the number of tens of thousands or thousands of thousands. Only when the point target echo simulation is right, the generated SAR echoes can be utilized to effectively verify imaging algorithms. Due to the fact that BP algorithm has the advantages of no-distortion and large depth of field, we choose BP algorithm to deal with imaging processing and validating the correctness of SAR echo simulation according to the final imaging results, of which the point target imaging results will be discussed in (4). The imaging performances of the distributed scene targets can be analyzed in two aspects: the whole performance of the SAR image and the focusing performance of the strong scatter targets. The entropy and contrast are indicators of the overall focusing performance of the SAR image—the smaller the entropy, the better the focusing performance; the greater the contrast, the better the focusing performance. Performances of the strong scatters in the SAR image are comprehensively analyzed in (4).

C. Simulation of SAR Imaging Algorithm and Verification of Real SAR Data

This process is consisted of point target simulation, distributed scene target simulation and verification by real data processing, mainly considering the scope of imaging algorithm application, such as imaging occasion, the approximation degree of the specific algorithm and the scope of the illuminated area. Real data are acquired by the SAR platform working in actual circumstances, and the true trajectory is unknown. However, the simulation data are generated with artificial parameters, and the trajectory of the SAR platform is given.

Under the no-motion-error condition, point target simulation plays an important role in the verification of SAR imaging algorithm, being able to reveal the potential problems and correctly reflecting defects hidden in the algorithm. At this moment, we can set breaking points in the program and perform the preliminary judgment according to the point target processing results after some specific operations. To evaluate of the performance of the point target imaging, two aspects should be considered: the focusing effect and the focusing position. No matter frequency domain algorithms or time domain algorithms are adopted, the focusing effects of the scene center are always standard. It should be noted that in time domain algorithms, the intervals of the neighbouring image grid must be less than the corresponding range resolution and azimuth resolution in the value. Also, the suitable values of the differences in both the range and azimuth dimensions need being experimented many times so that they can make a contribution to the focused image. Meanwhile, we should take into account the pixel range of the image grid and the covered scope of the image grid to ensure that all the point targets are included and that their position errors are small. For the verification of frequency domain algorithms, the two-dimension spectrum should not be folded, i.e., the Doppler bandwidth of the signal is less than PRF. More important, when interpolation [3] is necessary, the spectrums of the signal before and after the interpolation should not be folded in either the range dimension or the azimuth dimension. Furthermore,

the sampling rate changes in the corresponding dimension because of the interpolation, bringing changes to the pixel intervals of the image grid as well as the imaging scope. So we should calculate them once again. As to the determination of the effective imaged scene scope, we can distribute point targets in the region far away from the scene center and then evaluate the focusing performance through the final results. In addition, we can validate the focusing performance with the help of the information about the approximation degree of the common algorithms, which requires that we have a good knowledge of the specific algorithm and that we calculate the reasonable approximation according to real conditions.

From the above, the verifications of distributed scene target simulation and real data processing can be fulfilled by two aspects: the whole focusing effect of the SAR image and the very focusing effect of the strong scatters.

D. Evaluation of SAR Imaging Results

The quality verifications of SAR imaging results can be comprised of three aspects: point target imaging, distributed scene target imaging as well as real data processing. By analyzing the corresponding indicators, we can reasonably judge the image quality.

In the broadside mode, the pulse response function (IRF) of point target appears as the ‘sinc’ shape in both the range and azimuth dimensions for narrowband SAR. Impulse response width (IRW), normalized peak side-lobe ration (PSLR) and normalized integrated side-lobe ratio (ISLR) are the main indicators of point target simulation. IRW refers to 3dB main-lobe width of IRF, i.e., the resolution of the image. PSLR signifies the ratio of first side-lobe to the main-lobe, representing as decibel (dB). ISLR denotes the ratio of the energy of all side-lobes to the energy of the main-lobe, which can be expressed as

$$ISLR = 10 \log_{10} \left[\frac{(P_{total} - P_{main})}{P_{main}} \right] \quad (1)$$

where P_{main} is the power of the main-lobe, and P_{total} is sum of the main-lobe power and all the side-lobe power. In the broadside mode of narrowband SAR, the IRF of point target is centered exactly on the middle line of the main-lobe; the theoretical values of normalized PSLR and ISLR are about -13.25dB and -9.98dB, respectively. For the scene center point target, if its IRFs are not symmetric or normalized PSLR/ISLR deviates from the theoretical value, there would be problems existing in the imaging algorithm.

For distributed scene target simulation results, it is a necessity to calculate the entropy and contrast. Then, the obtained values are compared with the corresponding ones of the original image, respectively. Generally speaking, the smaller the difference between the two entropies as well as the difference of the two contrasts, the better the distributed scene target simulation. For strong scatters within the sub-scene, we can choose the range bin containing this scatter and extract the region where the scatter locates. Then interpolation is performed to get the IRF of this point target. Determining the IRW, PSLR and ISLR values, we can compare them with the corresponding values of the original image. The little the

difference of each corresponding values, the better the focusing performance of the strong scatters.

For the verification of the real SAR data processing, we can extract part region of the specific range bin containing two corner reflectors in the azimuth dimension. After performing interpolation, we can determine the resolution of the SAR image by judging whether the main-lobes of the two corner reflectors are separated. Besides, we can perform interpolation on the region where a single corner reflector is located, and then obtain the IRF, calculate the IRW, PSLR as well as ISLR. The windowing function is usually applied to suppress the influences of noise or clusters when range compression and azimuth compression are performed, which may result in a normalized PSLR value less than -20dB and a normalized ISLR value less than -17dB.

III. EXPERIMENTAL RESULTS

In this part, different simulations and real data experiments are performed to analyze the SAR system parameter design, to quickly generate SAR echoes via ICCM, to simulate the SAR imaging algorithms and deal with real data and to quantitatively evaluate the imaging results. The consequential results are utilized to validate the correctness and effectiveness of the proposed testing method.

A. Validation of Selected PRF Value in SAR Systems Mounted on High-maneuvering Platform

The known parameters are listed in the following: radar carrier center frequency $f_c = 16GHz$, the antenna elevation aperture length $D_r = 0.36m$, the antenna azimuth aperture length $D_a = 0.8m$, the height of the platform $H = 80km$, the swath width $W = 6km$, the range to the scene center line $R_s = 139.4757km$, the velocity of the platform $v = 8 \times 10^3 m/s$. Verify that $PRF = 22000Hz$ is satisfying.

The PRF value should satisfy the following three constraints:

1) The Doppler bandwidth can be approximately expressed as $B_d = 2v/D_a = 20000Hz$. Generally, the PRF value should keep a surplus capacity of 10% and we have $PRF \geq 1.1B_d = 22000Hz$.

2) To avoid swath ambiguity, that is, the magnetic signal cannot be transmitted until the former one is received, the subsequent condition should be satisfied: $2W \cos \theta / c < 1/PRF = PRT$. Thus, we have

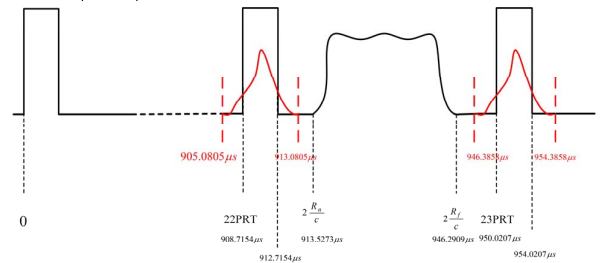


Fig. 1 Sequence chart of SAR signal

$PRF < c/[2W \cos d(35)] \approx 30519.3647Hz$, where ∂ is the complement angle of the incident angle and $\partial = \pi/2 - \cos^{-1}(H/R_s)$; PRT denotes the pulse repeat time and $c = 3 \times 10^8 m/s$ represents the velocity of the magnetic wave.

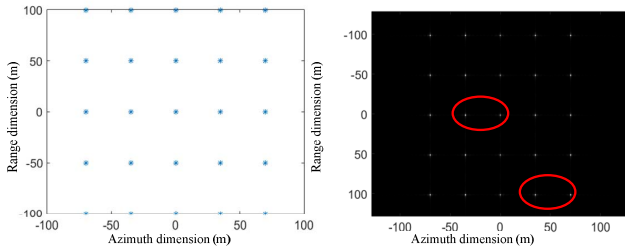
3) It is a necessity to avoid that the time period singularity echoes occur mixes with the received echoes. Now we draw the sequence chart of the SAR signal, as shown in Fig. 1, where the “rectangular” denotes the transmitted signal, the “peak” represents the singularity echo, and the time interval $[2R_n/c, 2R_f/c]$ (R_n and R_f are short and long range, respectively) signifies the SAR echoes. Apparently, the parameter $PRF = 22000Hz$ meets the design requirement of high-maneuvering SAR platforms.

B. Validation of SAR Echo Simulation

In order to validate the correctness of SAR echo simulation, we design simulation experiments of point targets and distributed scene targets.

1) verification by point target simulation

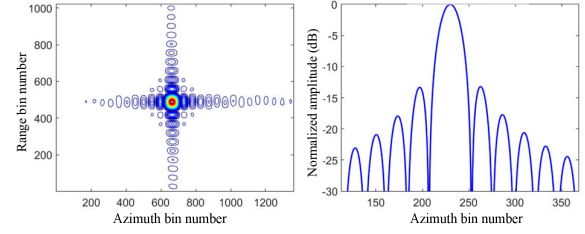
According to the parameters in Table 1, we distribute the point targets on the ground with the distance of 30m in the azimuth dimension and the distance of 50m in the range dimension, as Fig. 2(a) shows. The ICCM is adopted to generate SAR echoes of 25 point targets with a high speed as well as a high accuracy. To verify the correctness of the generated echoes, BP algorithm is utilized to deal with imaging processing, and Fig. 2(b) is thus obtained. The theoretical values of the range resolution and the azimuth resolution are 1.36m and 0.70m, respectively. To validate the feasibility of the generated SAR echoes, the imaging result analysis of the point targets is employed to evaluate the performance. The two point targets enclosed in the ellipse are chosen and two-dimension interpolations are performed, separately. Thus, we obtain the corresponding contour maps, IRFs in both the range dimension and the azimuth dimension, as shown in Fig. 3. For narrowband SAR imaging, the contour maps of point targets are cross-shaped in the range and azimuth dimension when the SAR platforms bear a constant velocity along a straight line. Additionally, the IRFs in both the range and azimuth dimension are presented as a standard “sinc” function with normalized PSLR value -13.25dB and ISLR value -9.98dB, respectively. By calculating the PSLR, ISLR and IRW of the



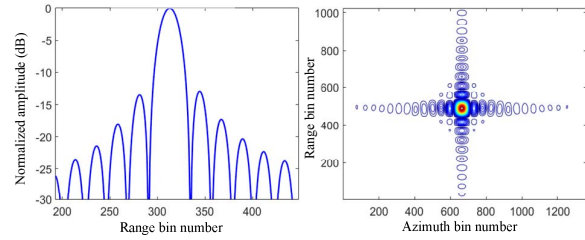
(a) Sketch map of point targets (b) Imaging result by BP algorithm
Fig. 2 Sketch map and imaging result of point targets

Table 1 SIMULATION PARAMETERS

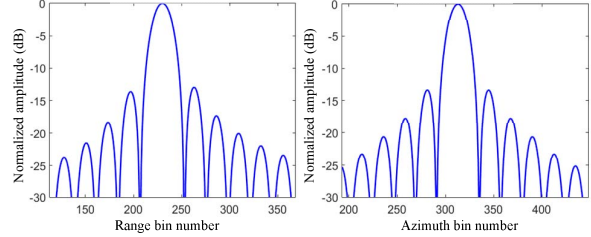
Parameter	Wave-length	pulse width	Band-width	PRF	velocity	Shortest range
Value	3 cm	24 μs	110MHz	1000Hz	75 m/s	12 km



(a) Contour map of scene center point (b) IRF profile along the range dimension



(c) IRF profile along the azimuth dimension (d) Contour map of scene edge point



(e) IRF profile along the range dimension (f) IRF profile along the azimuth dimension

Fig. 3 Contour maps, IRF profile maps along the range dimension and IRF profile maps along the azimuth dimension of point targets after interpolation

IRFs, we achieve the quantitative results in Table 2. Evidently, the two point targets focus well and their IRFs in both range and azimuth dimensions are centered on the middle line of the main-lobe. Furthermore, the corresponding normalized PSLR, ISLR and IRW are close to the standard values.

Table 2 RESULT ANALYSES OF POINT TARGETS IN BOTH RANGE AND AZIMUTH DIMENSIONS

Result Analyses	Range			Azimuth		
	PSLR (dB)	ISLR (dB)	IRW (m)	PSLR (dB)	ISLR (dB)	IRW (m)
Scene center point	-13.25	-9.98	1.35	-13.26	-9.97	0.69
Scene edge point	-13.28	-10.01	1.35	-13.27	-10.02	0.69



(a) Original SAR image



(b) Imaging result of distributed scene targets by ICCM

Fig. 4 Simulation results of distributed scene targets

2) verification by distributed scene target simulation

Fig. 4(a) shows the original SAR image, which provides the gray value information for echo generation. The ICCM is utilized to accomplish the distributed scene target echoes. Then, BP algorithm is adopted to achieve the imaging results, as shown in 4(b). The entropy of Fig. 4(a) is 14.86, and the corresponding contrast is 0.89. For comparison, the entropy of Fig. 4(b) is 14.88, and its contrast is 0.88. Intuitively, both the entropies and the contrasts of the original SAR image and the simulated SAR image are very close, respectively. As a result, the performances of the imaging results are very close, which validate the feasibility of the distributed scene targets simulation via the ICCM.

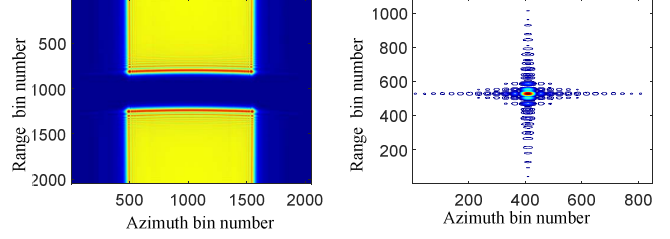
C. Verification by SAR Imaging Algorithm Simulation

In this part, point targets, uniformly distributed with a distance of 100m in both the range and azimuth dimension as Fig. 2(a) reveals, are dealt with by the improved range migration algorithm (RMA) [16] with the parameters in Table 3.

Fig. 5 (a) represents the two-dimension spectrum of the scene center point target after modified stolt interpolation (MSI) within the improved RMA. Fig. 5(b) shows the contour map with respect to Fig. 5(a). Obviously, the two-dimension spectrum is folded in the range dimension, and the resultant normalized PLSR and ISLR in the range dimension are -7.08dB and -3.25dB in the listed order, which demonstrates an inferior imaging performance. This is because the sampling rate changes after MSI. Now the two-dimension spectrum in the range dimension broadens so greatly that it exceeds the sampling rate of the original signal

Table 3 SIMULATION PARAMETERS

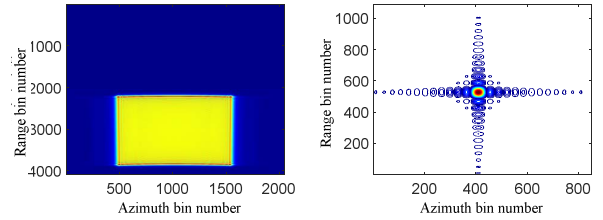
Parameter	Wave-length	Pulse-width	Band-width	Sampling rate	PRF	Shortest range
Value	3 cm	6 μ S	150MHz	180 MHz	400Hz	16 km



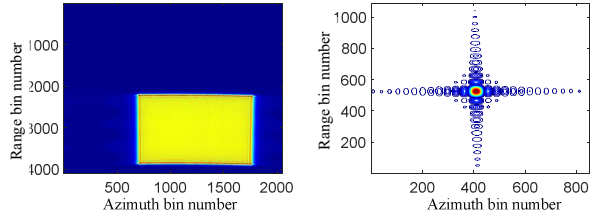
(a) Two-dimension spectrum (b) Contour map of scene center point
Fig. 5 two-dimension spectrum and contour map of scene center point without range upsampling

and folds in the range dimension, which ultimately causes defocusing. Therefore, the upsampling in the range dimension should be performed before the MSI to increase the sampling rate in the range dimension and to avoid the folding of the two-dimension spectrum in the range dimension. This operation aims to improve the range sampling rate by means of signal processing, without actually increasing the system's sampling rate.

Fig. 6(a) and Fig. 7(a) give the two-dimension spectrums of scene center point and scene edge point, respectively, which are obtained with zero padding (the number of zero padding is the same as the length of the signal in the range dimension) in the range frequency domain before the MSI. Correspondingly, the contour maps are depicted in Fig. 6(b) and Fig. 7(b). It is shown that the two-dimension spectrums do not fold in the range dimension. Moreover, the normalized PLSR, ISLR values of the scene center point target and the scene edge point target in both the range dimension and the azimuth dimension are presented in Table 4, which demonstrates that the imaging algorithm has a good performance and the point targets focus well.



(a) Two-dimension spectrum (b) Contour map of scene center point
Fig. 6 Two-dimension spectrum and contour map of scene center point with range upsampling



(a) Two-dimension spectrum (b) Contour map of scene edge point
Fig. 7 Two-dimension spectrum and contour map of scene edge point with range upsampling

Table 4 RESULT ANALYSES OF POINT TARGETS IN BOTH RANGE AND AZIMUTH DIMENSIONS

Result Analyses	Range		Azimuth	
	PSLR (dB)	ISLR (dB)	PSLR (dB)	ISLR (dB)
Scene center point	-13.28	-10.04	-13.29	-10.04
Scene edge point	-13.29	-10.11	-13.29	-10.04

D. Verification by Real SAR Data Processing

In this part, we get a real SAR data processing result, as illustrated in Fig. 8. Magnifying the sub-scene C, we obtain Fig. 9, where the two adjacent corner reflectors, with a distance of 0.25m in the azimuth dimension, are included in the ellipse. To evaluate the resolution performance of the adopted algorithm, we should take further analyses of the targets in the ellipse with the help of interpolation, more clearly displaying the two targets. In Fig. 10, the main-lobes of the two corner reflectors have almost been separate with each other. Also, the side-lobe is about 30dB lower than the main-lobe (because of the windowing operation so as to suppress the side-lobes), which indicates that the adjacent corner reflectors achieve well resolution in the azimuth dimension.

IV. CONCLUSION

This paper presents a novel testing method for narrowband SAR imaging algorithms in the broadside mode, which



Fig. 8 SAR imaging result

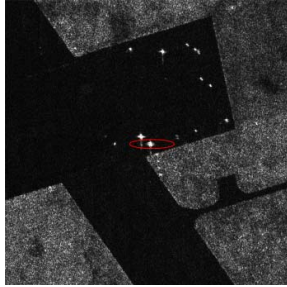


Fig. 9 Magnified result of sub-scene C

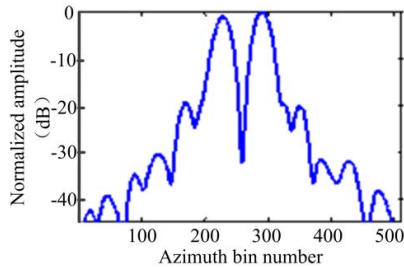


Fig. 10 IRF of adjacent targets along the azimuth dimension contained in the ellipse

roundly validates the correctness of SAR imaging algorithms and improves the effectiveness of algorithm testing effort from four aspects: system parameter design, SAR echo simulation, verifications of SAR imaging algorithms and evaluations of SAR imaging results. In addition, it should be noted that the effect verification of SAR imaging results is applicable for narrowband SAR imaging algorithm in the broadside mode, and its evaluation indicators are totally different from those of the ultra-wideband SAR imaging algorithms, which will be further studied in the next step. However, in the squinted mode, the range cell migration will be more serious and the imaging algorithms more complex. Still, the IRFs in both range and azimuth dimensions are not likely to be distributed in a single range or azimuth bin. More factors should be taken into account and the testing for squinted SAR imaging algorithms will be the research focus in the next step.

ACKNOWLEDGMENT

The authors would like to thank the anonymous reviewers for their valuable comments to improve the quality of study.

REFERENCES

- [1] I. G. Cumming, F. H. Wong, Digital Processing of Synthetic Aperture Radar Data: Algorithm and Implementation. Boston, MA: Artech House, 2005.
- [2] W. G. Carrara, R. S. Goodman, R. M. Majewski, Spotlight Synthetic Aperture Radar: Signal Processing Algorithm. Boston, MA: Artech House, 1995.
- [3] H. L. Li, Study on Fast Back-Projection Algorithms for Airborne SAR Imaging. Xi'an: Xidian University, 2015.
- [4] S. M. Zhu, Software Testing Method and Technology. Beijing: Tsinghua University Press, 2014.
- [5] X. H. Yang, How to Enhance the Value of Software Testing. Beijing: China Machine Press, 2016.
- [6] G. J. Myers, T. Badgett, C. Sandler, The Art of Software Testing. Hoboken, New Jersey: John Wiley & Sons, Inc., 2012.
- [7] P. C. Jorgensen, Software Testing: A Craftsman's Approach. Boca Raton: CRC Press, 2013.
- [8] A. Tarlinder, Developer Testing: Building Quality into Software. Addison-Wesley, 2016.
- [9] E. T. Barr, M. Harman, P. Mcminn, M. Shahbaz, and S. Yoo, "The oracle problem in software testing: a survey," IEEE Trans. Softw. Eng., vol. 41, pp. 507-525, May 2015.
- [10] M. Harman, A. Mansouri, and Y. Y. Zhang, "Search based software engineering: Trends, techniques and applications," ACM Computing Surveys (CSUR), vol. 45, pp. 1-61, November 2012.
- [11] A. D. Neto, R. Subramanyan, M. Vieira, G. H. Travassos, and F. Shull, "Improving evidence about software technologies: a look at model-based testing," IEEE Soft., vol. 25, pp. 10-13, May 2008.
- [12] J. Itkonen, M. V. Mantyla, and C. Lassenius, "The role of the tester's knowledge in exploratory software testing," IEEE Trans. Softw. Eng., vol. 39, pp. 707-724, May 2013.
- [13] A. Bertolino, "Software Testing Research: Achievements, Challenges, Dreams," in IEEE Future of Softw. Eng. (FOSE'07), Minnesota: Academic, May 2007, pp. 85-103.
- [14] G. B. Jing, Y. J. Zhang, Z. Y. Li, G. C. Sun, M. D. Xing, and Z. Bao, "Efficient realization of SAR echo simulation based on GPU," Syst. Eng. and Electron., vol. 38, pp. 2493-2498, November 2016.
- [15] Y. Y. Huai, Y. Liang, M. D. Xing, L. T. Zeng, and Z. Y. Li, "An inverse extended omega-K algorithm for SAR data simulation with trajectory

deviations,” IEEE Geosci. Remote Sens. Lett., vol. 13, pp. 826-830, June 2016.

[16] L. Zhang, J. L. Sheng, M. D. Xing, Z. J. Qiao, T. Xiong, and Z. Bao, “Wavenumber-domain autofocusing for highly squinted UAV SAR imagery”, IEEE Sensors J., vol. 12, pp. 1574-1588, May 2012.